

COMPARISON OF SPLITTING PROPERTIES OF VARIOUS 1×16 SPLITTERS

Catalina BUTSCHER^{1,2}, Dana SEYRINGER¹, Michal LUCKI²

¹Research Centre for Microtechnology, Vorarlberg University of Applied Sciences,
Hochschulstrasse 1, 6820 Dornbirn, Austria
²Department of Telecommunication Engineering, Faculty of Electrical Engineering,
Czech Technical University in Prague, Technicka 2, 16627 Prague 6, Czech Republic

catalina.burtscher@fhv.at, dana.seyringer@fhv.at, luckimic@fel.cvut.cz

DOI: 10.15598/aeec.v15i1.2014

Abstract. *Optical Access Networks (OAN) mostly use optical splitters to distribute the services from Optical Line Terminal (OLT) on the provider's side to the subscribers in Optical Network Unit (ONU). Optical splitters are the key components in such access networks as for example GPON and XG-PON by ITU-T. In this paper we investigate the optical properties of 1×16 Y-branch splitter and 1×16 MMI splitters based on different widths of multimode interference section and different lengths of the output ports. These two splitters were designed, simulated and the obtained results of both were studied and compared with each other. Additionally, we show that the used standard waveguide core size (usually $6 \times 6 \mu\text{m}^2$ to match the diameter of the single mode input/output fibers, i.e. to keep the coupling losses as low as possible) supports not only propagation of the single mode but of the first mode too, leading to an asymmetric splitting ratio (increasing non-uniformity of split power over all the output waveguides). Decreasing waveguide core size, it is possible to suppress presence of the first mode and this way to reduce non-uniformity.*

Keywords

GPON, MMI splitter, multimode interference splitter, Optical Access Networks (OAN), Optical Network Unit (ONU), optical splitting, XG-PON, Y-branch splitter.

1. Introduction

Optical splitters play an important role in the integrated optics allowing several customers to share the

same connection, bringing high-speed networking, digital television and telephone services to residences using fiber-optic cables [1].

There are two main approaches used to split one optical signal into N output signals. One of these approaches is to use a MultiMode Interference (MMI) coupler, where the splitting of the optical signal is based on a self-imaging effect [1] and [2]. MMI splitters feature a large splitting number and a stable splitting ratio, ensuring good uniformity over all output signals [3]. They exhibit good fabrication tolerance since the splitting is performed in a large multimode section. However, their main disadvantage results from the fact that the length of the MMI section is wavelength-dependent, i.e. MMI splitters are designed solely for one wavelength and can only operate in a narrow wavelength band. They are also polarization-dependent, but it was shown that for strong guidance waveguide structures this dependence is negligible [4].

Another possibility to split an optical signal is to make it as a cascade of one-by-two waveguide branches called Y-branch splitting. Y-branch splitters are the key components in Fiber-To-The-x (FTTx) networks because they are polarization and wavelength-independent, i.e. one device can be used in the whole operating wavelength window. However, they have the disadvantage that the processing of branching points, where two waveguides start to separate, is technologically very difficult, leading to an asymmetric splitting ratio of the split power over all the output waveguides. Furthermore, Y-branch splitters, especially high channel optical splitters, are much larger in comparison to MMI splitters.

In the MMI approach, optical properties of a splitter depend on the width of a multimode coupler. Therefore, in this paper we studied the splitting properties of

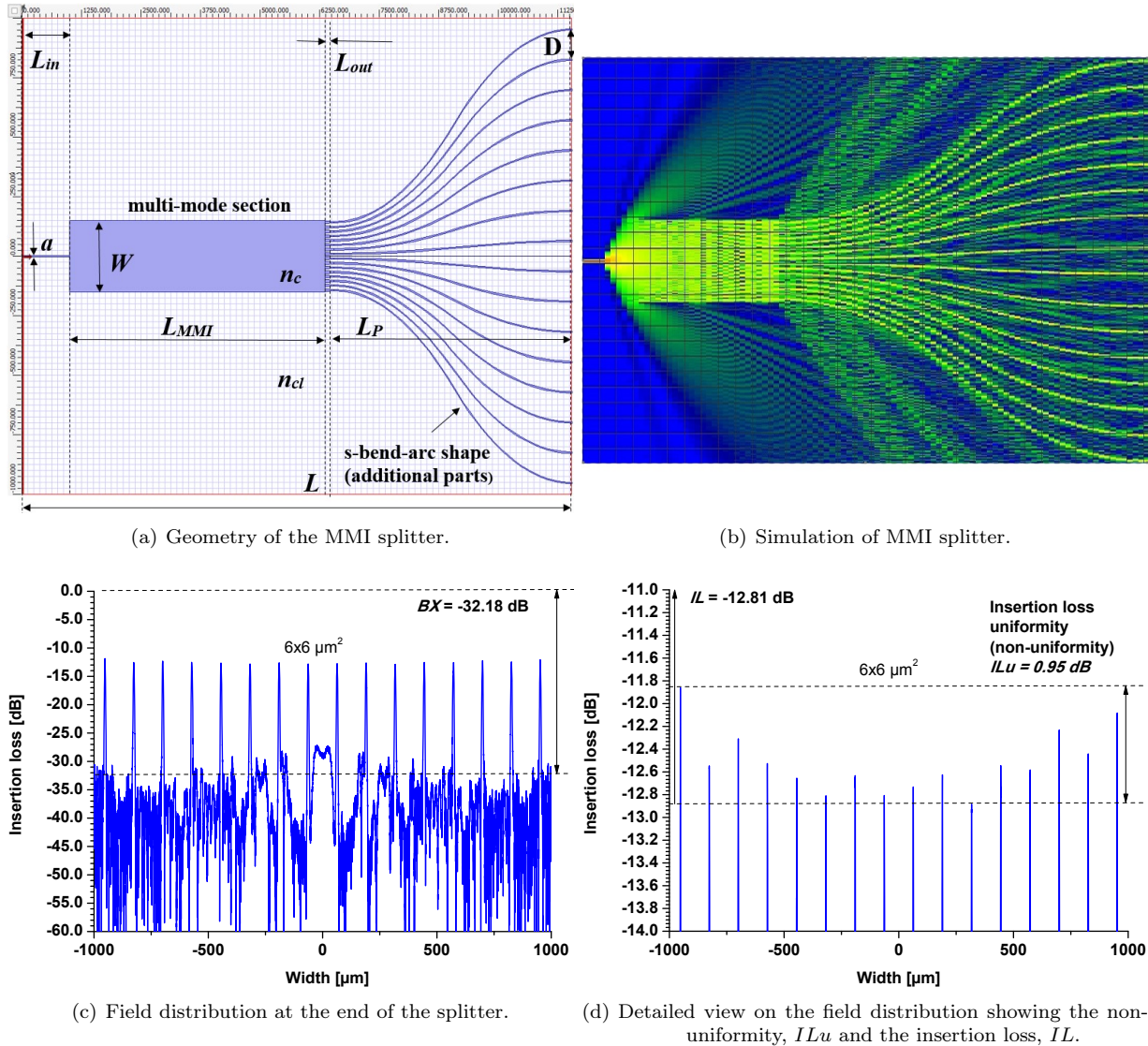


Fig. 1: 1×16 MMI splitter (Design 1).

1×16 MMI splitter in terms of different widths of the multimode interference section. The best 1×16 MMI splitter design was compared with 1×16 Y-branch splitter to show their advantages and disadvantages.

In Y-branch splitters, additionally, we show that not only technology but also the waveguide core size has strong influence on the non-uniformity of the split power.

2. Design and Simulation of 1×16 MMI Splitter

The 1×16 MMI splitter operating at wavelength $\lambda = 1550$ nm was designed and simulated using Optiwave tool (OptiBPM Designer using Beam-Propagation Method).

2.1. Design of 1×16 MMI Splitter

In Fig. 1(a) the geometry of 1×16 MMI splitter is shown together with its design parameters: n_{cl} - refractive index of the cladding, n_c - refractive index of the core, W - width of the MMI section, L_{MMI} - length of the MMI section, a - width of the input/output waveguides, L_{in} - length of the input waveguide, L_{out} - length of the tapered part of output waveguide, L_p - length of the output waveguides and D is the port pitch.

The design of the splitter was focused on weakly guiding glass waveguides with the refractive index of the cladding $n_{cl} = 1.445$ and of the core $n_c = 1.456$. The core size of the input/output waveguides was set to $6 \times 6 \mu\text{m}^2$ to support the single mode propagation only. To study the properties of the 1×16 MMI splitter the width of the multimode section, W was set to

Tab. 1: Comparison of splitting parameters of 1×16 MMI splitter for the different widths of multimode section and different lengths of the output ports.

Design	W (μm)	LMMI (μm)	L_p (μm)	Non-uniformity ILu (dB)	Insertion loss, IL (dB)	Background noise, BX (dB)	Length of, splitter, L (μm)
D1	200	2458	5000	0.95	-12.81	-32.18	8638
D1	200	2458	7500	1.04	-12.83	-36.85	11138
D1	200	2458	10000	1.28	-12.80	-37.72	13638
D2	300	5368	5000	0.51	-12.54	-36.8	11548
D2	300	5368	7500	0.39	-12.56	-37.71	14048
D2	300	5368	10000	0.26	-12.44	-41.35	16548
D3	400	9529	5000	0.92	-12.93	-35.06	15709
D3	400	9529	7500	0.61	-13.27	-32.76	18209
D3	400	9529	10000	0.57	-12.89	-33.21	20709
D4	500	14932	5000	1.72	-14.89	-37.69	21112
D4	500	14932	7500	1.91	-14.44	-30.17	23612
D4	500	14932	10000	0.83	-13.85	-33.63	26612

200 μm (Design 1 = D1), to 300 μm (Design 2 = D2), to 400 μm (Design 3 = D3) and finally to 500 μm (Design 4 = D4). The length of the MMI section, LMMI has varied from 2458 μm to 5368 μm , to 9529 μm and to 14932 μm . The length of the output waveguides, L_p was tested for different lengths, as 5000 μm , 7500 μm and 10000 μm . The length of the input port L_{in} was set to 1000 μm and the length of the tapers, L_{out} was 180 μm . The pitch of the output ports, D was set to 127 μm . Several shapes of the output waveguides were tested (Optiwave photonics tool offers three different standard shapes: s-bend-sine, s-bend-cosine and s-bend-arc). The best results (lowest losses) were obtained using s-bend-arc shape. The lengths of the designed splitters are shown in Tab. 1.

2.2. Simulation of 1×16 MMI Splitter

Figure 1(b) shows the top view of the simulated 1×16 MMI splitter (design D1 with the length of the output waveguides, $L_p = 5000 \mu\text{m}$) performed in Optiwave tool. Figure 1(c) presents the simulation results of 1×16 MMI splitter, i.e. field distribution at the end of the simulated structure together with background noise parameter, $BX = -32.18$ dB. Figure 1(d) shows the detailed view of the field distribution with the non-uniformity parameter (difference between the highest and the lowest peak, also called insertion loss non-uniformity), $ILu = 0.95$ dB and insertion loss (the worst peak), $IL = -12.81$ dB.

3. Different Widths of MMI Section

1×16 MMI splitters with different widths, W of the MMI section and lengths, L_p of output ports were de-

signed and simulated. The simulated results are shown in Tab. 1.

3.1. Considering the Splitting Parameters

Non-uniformity ILu , insertion loss IL and background noise BX , the best results were obtained as expected when applying the longest output ports, $L_p = 10000 \mu\text{m}$ in all designs.

Namely, the design D2 reached the lowest background noise, $BX = -41.35$ dB, a non-uniformity, $ILu = 0.26$ dB and an insertion loss, $IL = -12.44$ dB. For the design D3 the background noise $BX = -33.21$ dB, the non-uniformity $ILu = 0.57$ dB and the insertion loss $IL = -12.89$ dB. In the case of design D4 the background noise $BX = -33.63$ dB, the non-uniformity $ILu = 0.83$ dB and the insertion loss $IL = -13.85$ dB. From the simulation results it can be concluded that the best splitting characteristics were obtained for the design D2 with the width of the MMI section, $W = 300 \mu\text{m}$.

3.2. Considering the Whole Length of the MMI Splitter

The simulation results, in the case of the shortest splitter, where the paramount design parameter, $L_p = 5000 \mu\text{m}$ in each design, are presented in Fig. 2. In the design D2 the whole length of MMI splitter reached $L = 11548 \mu\text{m}$ (see Tab. 1). The background noise, BX is -36.8 dB (see Fig. 2(a)), the non-uniformity, $ILu = 0.51$ dB and the insertion loss, IL is -12.54 dB (see Fig. 2(b)). For the design D3, the whole length of the splitter, $L = 15709 \mu\text{m}$. The background noise, $BX = -35.06$ dB (see Fig. 2(c)), the non-uniformity, $ILu = 0.92$ dB and the insertion loss, $IL = -12.93$ dB (Fig. 2(d)). D4 design reached the whole length of the

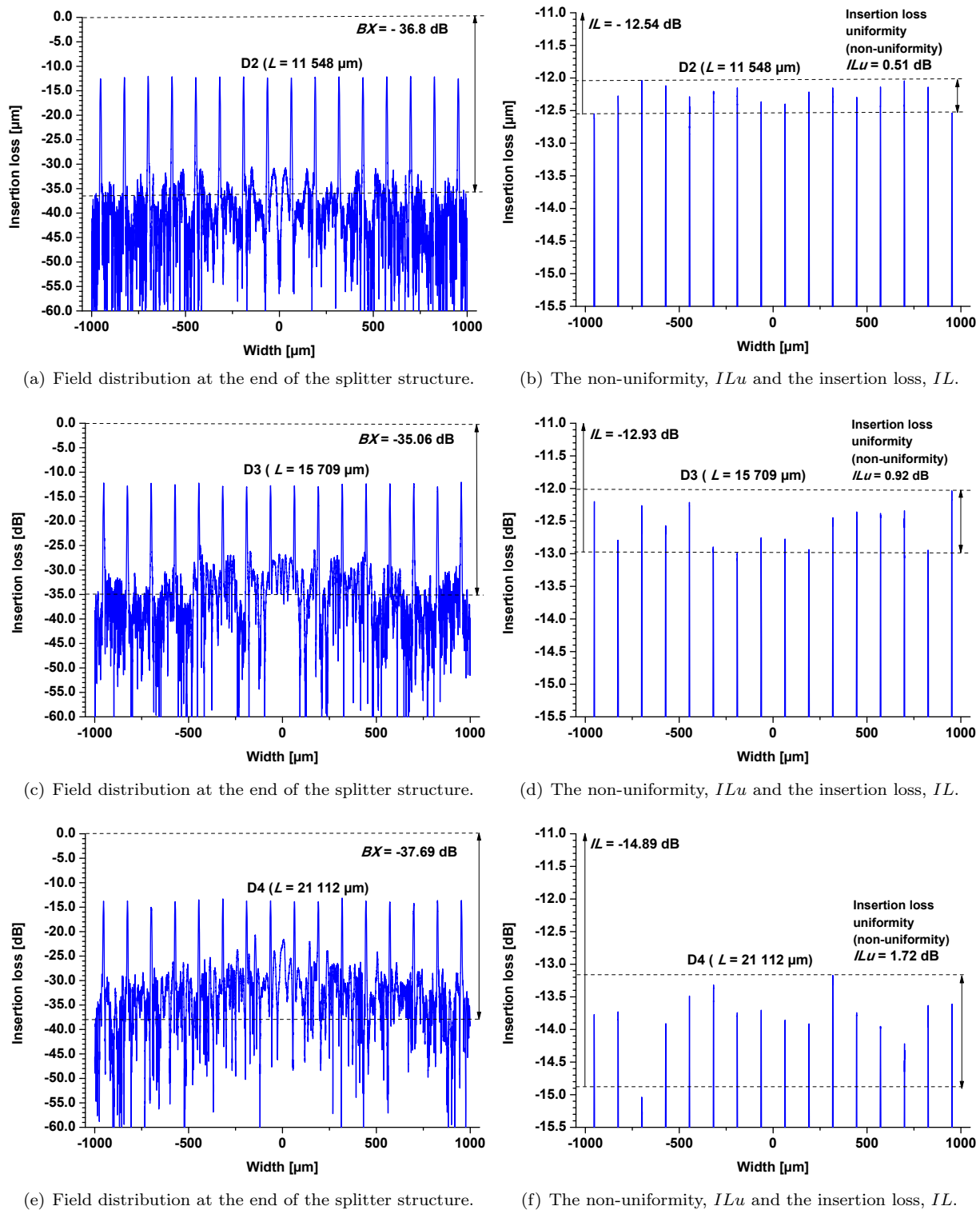


Fig. 2: Simulation results for different widths, W of MMI multimode section: field distribution at the end of the splitter structure (a), (c), (e) and detailed view of the field distribution showing the non-uniformity, ILu and the insertion loss, IL (b), (d), (f).

MMI splitter, $L = 21112 \mu\text{m}$. This splitter features the background noise, $BX = -37.69$ dB (see Fig. 2(e)), the non-uniformity, $ILu = 1.72$ dB and an insertion loss,

$IL = -14.89$ dB (see Fig. 2(f)). It is obvious from the simulation results that the design D2 reached the best optical splitting parameters.

Tab. 2: Comparison of splitting parameters of 1×16 Y-branch and 1×16 MMI splitters.

Y-branch		Non-uniformity ILu	Insertion loss IL	Background noise BX	Length of splitter L
	$6 \times 6 \mu\text{m}^2$	1.77 dB	13.09 dB	-49.04 dB	78000 μm
	$5.5 \times 5.5 \mu\text{m}^2$	0.89 dB	13.09 dB	-49.18 dB	78000 μm
MMI	$6 \times 6 \mu\text{m}^2$	0.51 dB	12.548 dB	-36.80 dB	11548 μm
	$5.5 \times 5.5 \mu\text{m}^2$	0.46 dB	12.432 dB	-36.84 dB	11548 μm

4. Design and Simulation of 1×16 Y-Branch Splitter

4.1. Design of 1×16 Y-branch Splitter

For the design of the 1×16 Y-branch splitter we used a Y-branch structure of 1×4 optical splitter as shown in Fig. 3(a). For the branches of this splitter a pre-defined "s-bend-arc" shape (OptiBPM tool) was used, because this shape provides the lowest losses [4]. The design of the 1×16 Y-branch splitter was constructed from two 1×4 Y-branch splitters connected by an additional branch to get 1×8 Y-branch splitter. Finally, two 1×8 Y-branch splitters were then connected to get the 1×16 Y-branch splitter. As can be seen from its geometry the splitter consists of a linear input port set to 1000 μm , 16 linear outputs and 15 branches, distributed on 4 layers (the length of the 1st branch layer, $L(1^{\text{st}}) = 5000 \mu\text{m}$, the 2nd branch layer is doubled, $L(2^{\text{nd}}) = 10000 \mu\text{m}$). To keep further the constant bending shape, the 3rd branch layer was also doubled i.e. $L(3^{\text{rd}}) = 20000 \mu\text{m}$ and the 4th branch layer, $L(4^{\text{th}}) = 40000 \mu\text{m}$. The output port's length was set to 2000 μm .

The pitch between the waveguides in each branch layer was automatically doubled, i.e. in the 1st branch layer $W(1^{\text{st}}) = 127 \mu\text{m}$, in the 2nd branch layer $W(2^{\text{nd}}) = 254 \mu\text{m}$, in the 3rd branch layer $W(3^{\text{rd}}) = 508 \mu\text{m}$ and in the 4th branch layer $W(4^{\text{th}}) = 1016 \mu\text{m}$. Thereby the whole length of the 1×16 Y-branch splitter reached 78000 μm and the width of the splitter was 1905 μm ($= 15 \times 127 \mu\text{m}$).

4.2. Simulation of 1×16 Y-branch Splitter

Figure 3(b) presents the top view of the simulated 1×16 Y-branch splitter using Optiwave tool. Figure 3(c) shows the corresponding field distribution at the end of the structures. The background noise of Y-branch splitter, $BX = -49.04$ dB (Fig. 3(c)). The uniformity of the split power over all the output channels, $ILu = 1.77$ dB and the insertion loss $IL = -13.09$ dB for Y-branch approach (Fig. 3(d)).

5. Optical Properties of 1×16 MMI and Y-Branch Splitters

MMI splitters have some advantages over Y-branch splitters. The main advantage is their low non-uniformity and size. The simulated results presented in the Tab. 2 confirm that for standard waveguide core (6×6) μm^2 the non-uniformity, $ILu = 0.51$ dB in case of MMI splitter is much lower than the non-uniformity, $ILu = 1.77$ dB for Y-branch splitter.

MMI splitter is approximately seven times shorter than the Y-branch splitter, namely 11548 μm in contrast to 78000 μm . Furthermore, the insertion loss, $IL = -12.548$ dB for MMI approach is slightly lower than insertion loss, $IL = -13.017$ dB for Y-branch splitter. On the other hand, the background noise of MMI splitter, $BX = -36.8$ dB is considerably higher than background noise of Y-branch splitter, $BX = -49.04$ dB. Insertion loss, $IL = -13.017$ dB for Y-branch splitter is slightly higher than for MMI splitter, where $IL = -12.548$ dB.

The deep study of the achieved simulation results summarized in Tab. 2 showed that in the standard (6×6) μm^2 waveguide not only propagation of the single mode is supported but also the presence of the first mode is already so strong that it causes additional asymmetric splitting of the optical signal at the branching points in Y-branch splitters. This becomes a dominant factor, particularly when reducing the length of the high channel Y-branch splitters [6]. To show this influence, we reduced the waveguide core size from (6×6) μm^2 to (5.5×5.5) μm^2 in both splitters, keeping the same size of the structures. The simulated results, namely the non-uniformity, ILu and insertion loss, IL of both splitters are shown in Fig. 4.

As can be seen in Fig. 4(b), the splitting parameters of the MMI splitter are only slightly improved since the splitting appears in the large coupler.

Y-branch splitter, consisting of many waveguides, features strong improvement of its optical properties, particularly the non-uniformity is strongly reduced from $ILu = 1.77$ dB (for (6×6) μm^2) to $ILu = 0.89$ dB (for (5.5×5.5) μm^2), that is less than one half of its original value (see Fig. 4(a)).

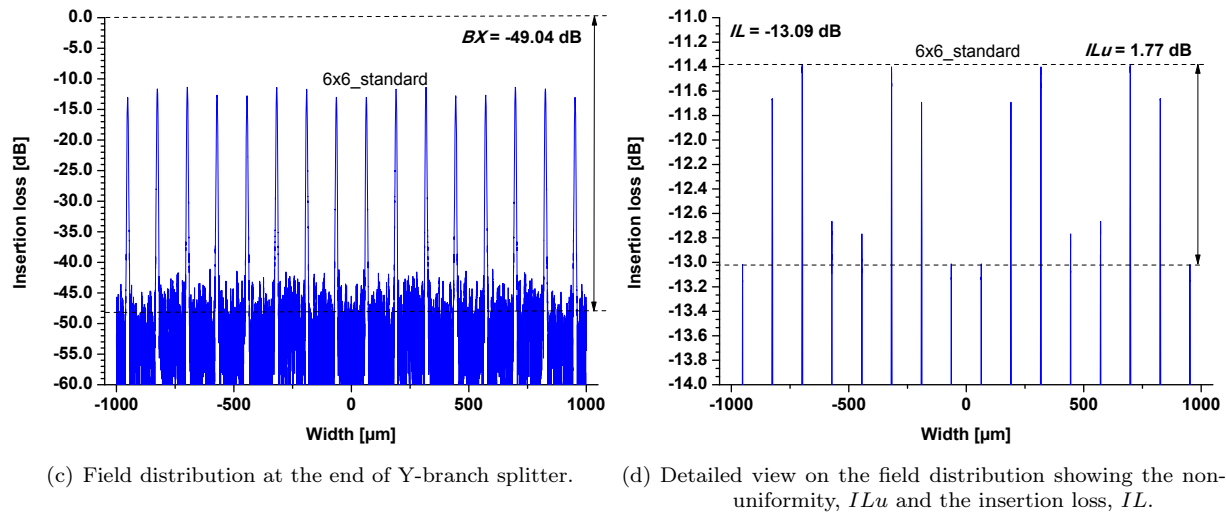
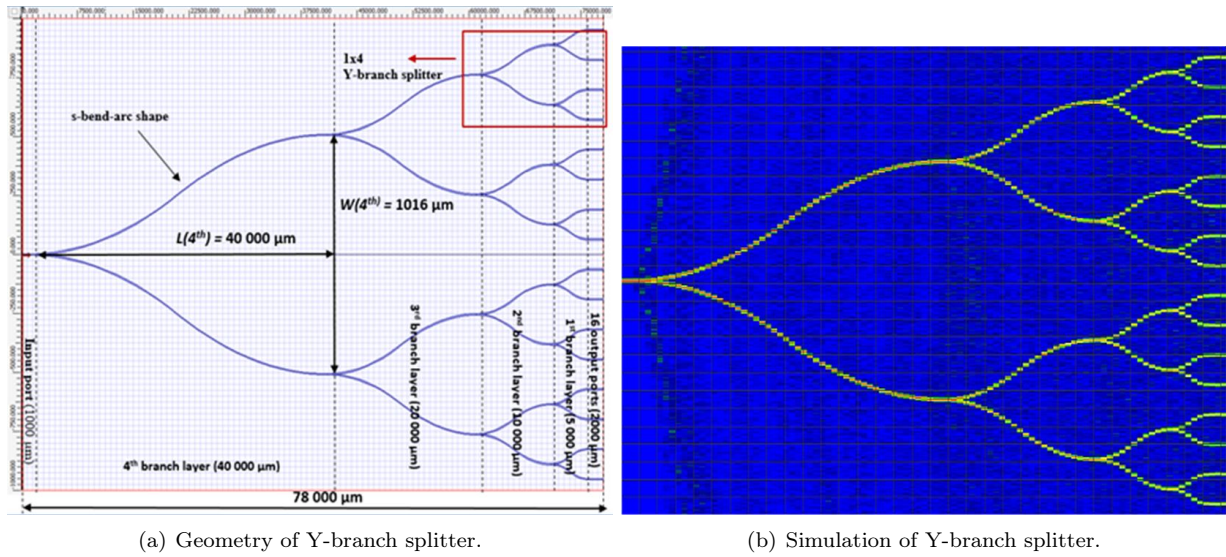


Fig. 3: 1×16 Y-branch splitter.

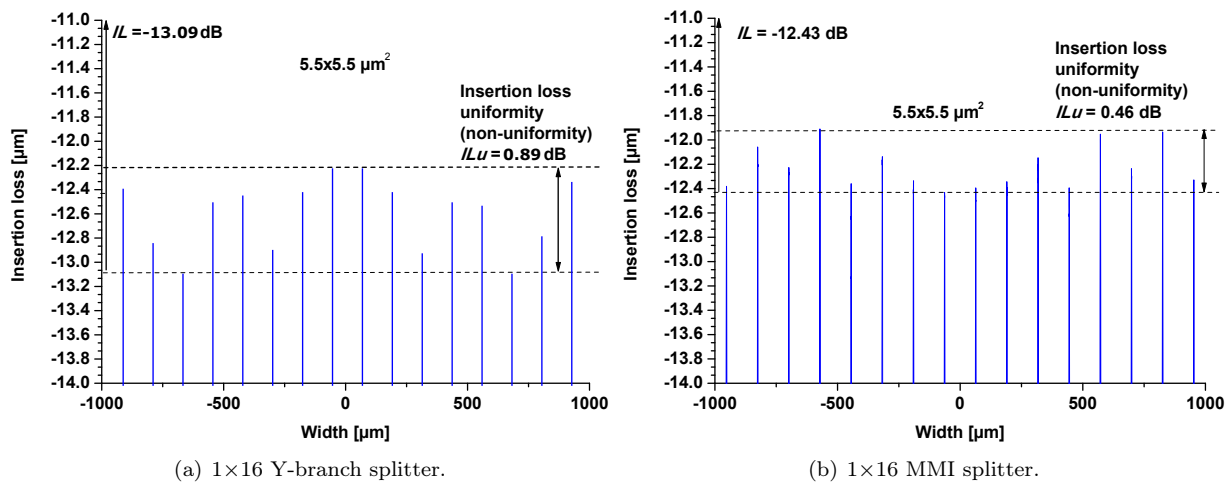


Fig. 4: Non-uniformity and insertion loss of 1×16 Y-branch splitter (a) and 1×16 MMI (b) splitters with the waveguide core size of $(5.5 \times 5.5) \mu\text{m}^2$.

6. Conclusion

In this paper we studied the optical properties of 1×16 MMI splitter based on different widths of MMI sections and 1×16 Y-branch splitter. It is evident from the simulation results that the width, W of the multimode interference section together with the lengths of the output ports are important design parameters. The simulation results showed that the optimal width of the MMI coupler, for which we were able to get the best performance of the MMI splitter, was obtained in D2 design. It was also showed that non-uniformity, IL_u and insertion loss, IL parameters can be improved when adjusting the length of the output waveguides, L_p . Additionally, by decreasing the waveguide core size it is possible to suppress the presence of the first mode and this way to reduce non-uniformity. Particularly, in the case of Y-branch splitter the non-uniformity is strongly reduced to less than one half of its original value. The comparison of all optical properties of both splitters using different waveguide cores is summarized in Tab. 2.

Acknowledgment

This work was supported by Czech Technical University student grant under the project SGS16/227/OHK3/3T/13.

References

- [1] KEISER, G. *FTTX Concepts and Applications*. 1st ed. New Jersey: Wiley-IEEE Press, 2006. ISBN 978-0-471-70420-1.
- [2] BRYNGDAHL, O. Image formation using self-imaging techniques. *Journal of the Optical Society of America*. 2015, vol. 63, iss. 4, pp. 416–419. ISSN 1084-7529. DOI: 10.1364/JOSA.63.000416.
- [3] KOHLER, L. *Study of optical splitters based on MMI and Y-branch approaches*. Austria, 2012. Master Thesis. Vorarlberg University of Applied Science Austria. Supervisor Dr. Dana Seyringer.

- [4] BACHMAN, M., M. K. SMITH, P. A. BESE, E. GINI, H. MELCHIOR and L. B. SOLDANO. Polarization-intensive low voltage optical waveguide switch using InGaAsP/InP four port Mach-Zender interferometer. In: *Conference on Optical Fiber Communication/International Conference on Integrated Optics and Optical Fiber Communication*. San Jose: Optical Society of America, 1993, pp. 32–33. ISBN 978-0780309982.
- [5] NOURSHARGH, M., E. M. STARR and T. M. ONG. Integrated Optic 1×4 splitter in $\text{SiO}_2/\text{GeO}_2$. *Electronics Letters*. 1989, vol. 25, iss. 15, pp. 981–982. ISSN 0013-5194. DOI: 10.1049/el:19890656.
- [6] BURTSCHER, C. *Design, Simulation and Optimization of High Channel Optical Splitters*. Austria, 2014. Master Thesis. Vorarlberg University of Applied Science Austria. Supervisor Dr. Dana Seyringer.

About Authors

Catalina BURTSCHER was born in Targoviste, Romania. She received her M.Sc. from the Vorarlberg University of Applied Sciences in 2014. Since 2014 she has been a Ph.D. student at the Czech Technical University in Prague. Her research interests include integrated optic, passive optical components for telecommunication.

Dana SEYRINGER was born in Martin, Slovakia. She received her first Ph.D. in microelectronics from the Slovak University of Technology in Bratislava in 1996, and her second Ph.D. at the Johannes Kepler University in Linz, Austria, in 1998. She is internationally known for her work on simulation methods.

Michal LUCKI was born in Starachowice, Poland. He received his first Ph.D. in microelectronics from the Czech Technical University in Prague in 2007. His research interests include photonics, photonic crystal fibers, optical network, telecommunication.